A Hybrid FEM-Based Procedure for the Scattering from Photonic Crystals Illuminated by a Gaussian Beam

Giuseppe Pelosi, *Fellow, IEEE*, Alessandro Cocchi, and Agostino Monorchio, *Member, IEEE*

***Abstract*—In this paper, we provide an efficient numerical procedure for evaluating the field scattered by two-dimensional (2-D) photonic crystals when they are illuminated by Gaussian beams. In particular, the incident Gaussian beam is interpreted as a spectrum of both homogeneous and inhomogeneous plane waves. The scattering of each plane wave is analyzed by resorting to a hybrid technique combining the finite-element method (FEM) with a Floquet modal expansion. Moreover, by applying the standard saddle point method, the evaluation of the field at a specific point of the exterior medium is reduced to the contribution of the fundamental Floquet mode of a single plane wave belonging to the incident spectrum, strongly enhancing numerical efficiency.**

***Index Terms*—Artificial crystals, electromagnetic scattering, FEM.**

I. Introduction

RECENTLY, the interest in photonic crystals has strongly increased due to the possibility of realizing structures with specific frequency selective properties [1]. Initial works on this subject focused on quantum electronic applications such as spontaneous emission inhibition [2], that plays a fundamental role in nano-cavity lasers [3] and in solar cells. If a photonic crystal is properly doped, a forbidden frequency band arises so that local modes can be trapped around the defects into the crystal lattice [4], [5]. In applied electromagnetics, photonic crystals have been used for realizing planar dielectric reflectors [6] and they have also been employed as substrates for dipoles and printed antennas to improve radiation performance [7], [8]. Their usage has also been prospected as stop-band filters in dielectric waveguides and patch antennas. In fact, photonic crystals differ from the typical dichroic surfaces because they preserve the same frequency selective properties independently on the polarization and direction of incident field [9], [10].

We note that several scattering problems presented in the literature on this topic have been limited to plane wave illumination conditions [6], [9], [10]. The purpose of this paper is to provide an efficient numerical procedure for evaluating the field scattered by such structures when they are illuminated by Gaussian beams. An exact solution can be provided by interpreting the incident Gaussian beam as a spectrum of both homogeneous and inhomogeneous plane waves. The scattering of each plane wave is analyzed by resorting to a hybrid technique combining the finite-element method (FEM) with a Floquet modal expansion [11], [12]. However, due to the particular properties of the photonic crystals, the evaluation of the field in the exterior medium under Gaussian beam illumination is reduced by applying the saddle point method to the contribution of the fundamental Floquet mode due to a single plane wave belonging to the incident field spectrum. This strongly increases numerical efficiency, actually limiting the computational time.

We note that spectral methods have been widely used in antenna problems in the context of high-frequency techniques for extending the validity of analytical solutions to the near field. First, the plane wave far-field transfer function of the structure is determined; then, this function is used as the kernel of a suitable spectral integral to reconstruct the proper Green's function of the problem [13]. In our case, the Green's function for the problem under investigation is obtained via a numerical procedure.

The paper is organized as follows. In the next section, we present the specific formulation for the scattering from a two-dimensional (2-D) photonic crystal illuminated by a Gaussian beam. In the same section, a hybrid technique FEM/Floquet modal expansion is employed to determine the far-field response of the structure to a simple plane wave illuminating the crystal. This plane wave far-field response is used to reconstruct the response of the system to a Gaussian beam illumination in the framework of a spectral method. In Section III, a high-frequency approximation is devised for the computation of the fields reflected from and transmitted through the 2-D photonic crystal. Numerical results will be shown in Section IV to demonstrate the effectiveness of the technique and to determine its limits of applicability. Finally, some concluding remarks are drawn in Section V.

II. Formulation

A. Incident Field Spectral Representation

Let us assume a 2-D photonic crystal that is periodic and infinite along the x direction of an orthogonal reference system, finite along the y direction, and homogeneous along the z direction, illuminated by a Gaussian beam $u^{\mathrm{inc}}(x,y)$ with arbitrary angular width and arbitrary mean incidence angle ϑ^i (Fig. 1). The case of TM_z polarization ($H_z = 0; u^{\mathrm{inc}} = E_z$) will be considered in the following, being the extension to the TE_z case ($E_z = 0; u^{\mathrm{inc}} = H_z$) straightforward. A harmonic time-dependence $\exp(j\omega t)$ is assumed and suppressed. The incident

Manuscript received August 5, 1998; revised August 9, 1999.

G. Pelosi and A. Cocchi are with the Department of Electronics and Telecommunications, University of Florence, I-50134 Florence, Italy.

A. Monorchio is with the Department of Information Engineering, University of Pisa, I-56126 Pisa, Italy.

Publisher Item Identifier S 0018-926X(00)05788-4.

Gaussian beam can be interpreted as a superposition of plane waves with the following spectral representation [14], [15]:

$$u^{\text{inc}}(x,y) = \int_{-\infty}^{+\infty} U^{\text{inc}}(x,y;\alpha)\,d\alpha = \int_{-\infty}^{+\infty} p(\alpha) f_\alpha(x,y)\,d\alpha \tag{1}$$

where $f_\alpha(x,y) = \exp[-j(\alpha x - \beta y)]$ denotes the phase factor, being β and α the wavenumber projection along x and y related to the free-space propagation constant k by $k^2 = \beta^2 + \alpha^2$; additionally, $k = 2\pi/\lambda_0$, λ_0 representing the wavelength of the incident field. Moreover, $p(\alpha)$ is the canonical Gaussian function

$$p(\alpha) = \frac{k}{a\sqrt{2\pi}} \exp\left[-\frac{a^2(\alpha-\bar{\alpha})^2}{2k^2}\right]. \tag{2}$$

In (2), a is a real positive number and $\bar{\alpha} = k\sin(\vartheta^i)$. We note that for the choice $k = a$, the incident field $u^{\text{inc}}(x,y)$ has unitary value at the origin of the coordinate system.

In (1), the integral is extended to the interval $]-\infty, +\infty[$; however, most of the energy of the incident field is comprised in the interval $[\bar{\alpha}-k, \bar{\alpha}+k]$, so that integration can be bounded to this interval. For out-of-normal incidence, $\bar{\alpha}$ assumes nonzero value: in this case, evanescent plane waves are present with propagation constant $|\alpha| > k$ propagating along x and attenuating along y. For an exact reproduction of the incident field, the plane waves with $|\alpha| > k$ should be included in the series; however, they become significant in the evaluation of the scattered field at distances lower than $\lambda/10$ from the air-photonic crystal interface, but they do not contribute appreciably to the correct value of the scattered field for greater distances. In this sense, they can be neglected without loss of accuracy as will be shown in Section IV.

A discretization of (1) can be performed if we consider a discrete summation of plane waves equally sampled in the variable α; in particular, the integral operator becomes a discrete series that can be cast in the following form:

$$u^{\text{inc}}(x,y) = \sum_{i=1}^{N+1} \frac{k}{a\sqrt{2\pi}} \exp\left[-\frac{a^2(\alpha_i-\bar{\alpha})^2}{2k^2}\right] \times \exp[-j(\alpha_i x - \beta_i y)]\Delta\alpha \tag{3}$$

where $\Delta\alpha = 2k/N$ is the sampling interval in the wavenumber domain, α_i and β_i define the direction of each single plane wave on the xy plane.

A discussion about the truncation number N of the series in (3) is in order. Equation (3) can be interpreted as a discrete representation of the integral function in (1) in the interval $[\bar{\alpha}-k, \bar{\alpha}+k]$; as it is well known from signal processing theory, when a continuous function is discretized, its Fourier transform becomes periodic and the sampling interval must be chosen in accordance with Shannon's theorem to avoid the "aliasing" error in the corresponding transform domain. The same problem occurs in our case if we consider that $p(\alpha)$ is the Fourier transform of $u^{\text{inc}}(x,y)$. In particular, by sampling the spectrum of the incident field, a *comb*-type field in the space domain is obtained so that the computation of the scattered field is corrupted by the presence of the fictitious side replicas. This problem is even worsened when we observe the scattered field at grazing angles with respect to the air-crystal interface. In Fig. 2 we show the Gaussian incident field obtained by setting either $N = 20$ (continuous line) or $N = 30$ (dashed line). In practical applications, accurate results are obtained if a high value is used for N (typically $N > 200$), substantially below the Shannon's sampling interval [15]. This results in a prohibitive computational cost for practical applications. However, as will be shown in Section III, the computational time can be drastically reduced by resorting to a high-frequency approximation.

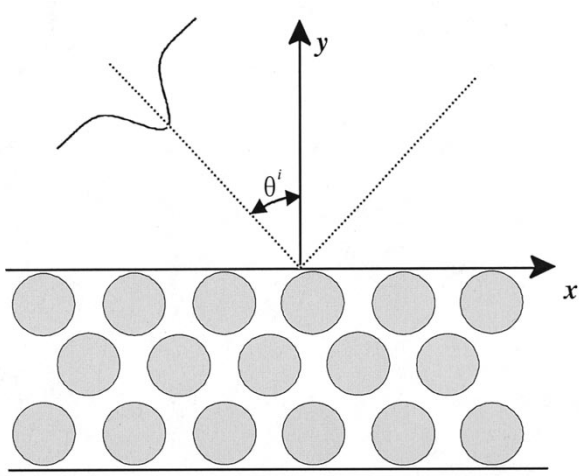

Fig. 1. Geometry of the problem: a Gaussian beam impinging on a photonic crystal.

B. FEM/Floquet Modes Procedure

By utilizing a spectral representation for the incident field, the scattering of a Gaussian beam from the photonic crystal can be analyzed by considering separately the scattering of both homogeneous and inhomogeneous plane waves $U^{\text{inc}}(x,y;\alpha) = p(\alpha)f_a(x,y)$. This problem can be solved by employing a hybrid technique utilizing the FEM in conjunction with a Floquet's modal expansion [11], [12]. We note that FEM is particularly suited to analyze this kind of structures that possess arbitrary shaped inhomogeneities: in fact, a conformal meshing of the geometrical features allows us to accurately resolve the fields within the crystal.

We start by considering the scattering from an infinite, 2-D periodic structure (Fig. 3) illuminated by a plane wave $U^{\text{inc}}(x,y;\alpha)$, which can be either homogeneous or inhomogeneous, impinging at an angle ψ that in the most general case is complex

$$U^{\text{inc}}(x,y;\alpha) = p(\alpha)e^{-j(\alpha x-\beta y)}\hat{z} \tag{4}$$

where $\alpha = -k\cos\psi$ and $\beta = k\sin\psi$.

Floquet's theorem dictates the periodicity of the scattered field along x; in particular, if d is the period along x, the scattered fields evaluated at x and $x+d$ are identical but for a phase factor $\exp(jkd\cos\psi)$. This allows us to determine the scattered field by analyzing a basic periodicity cell defined in

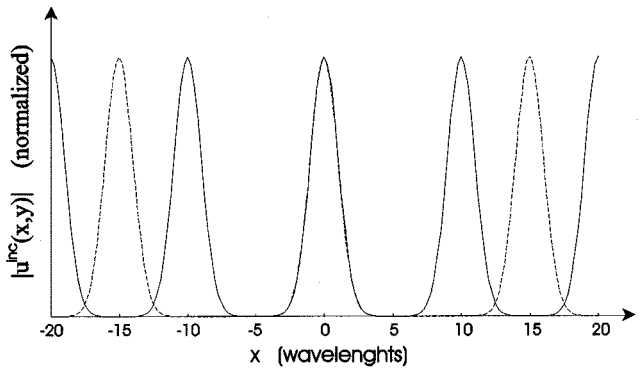

Fig. 2. Incident field representation obtained by using the inverse Fourier transform of the spectrum. Continuous line: $N = 20$; dashed line: $N = 30$.

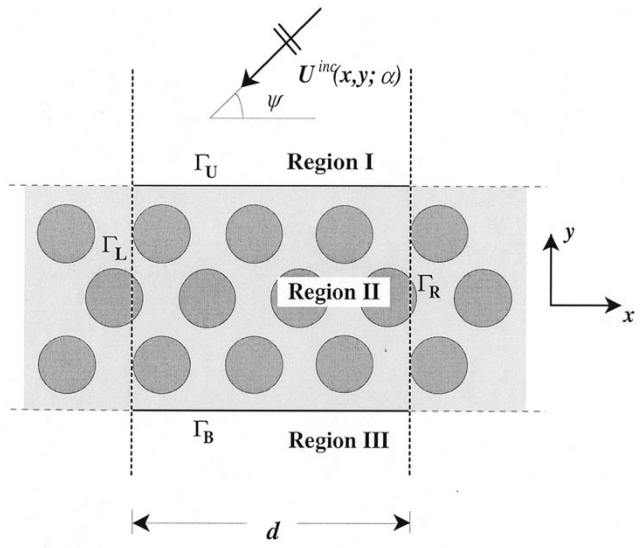

Fig. 3. Elementary problem: periodicity cell illuminated by a plane wave.

$(0 \le x \le d)$ and divided into the following regions: two unbounded regions I and III (Fig. 3) and a bounded region II defined in $(0 \le x \le d; y_U \le y \le y_B)$ and delimited by the boundaries $\Gamma_L, \Gamma_R, \Gamma_U$, and Γ_B.

In region I, the total field is given by the sum of the incident and the scattered fields $U^{\rm tot}(x,y;\alpha) = U^{\rm inc}(x,y;\alpha) + U^s(x,y;\alpha)$, while in region III, $U^{\rm tot}(x,y;\alpha) = U^{\rm tr}(x,y;\alpha)$, i.e., the total field coincides with the transmitted field. Each spectral component of the scattered field can be expanded in terms of Floquet modes as

$$U^s(x,y;\alpha) = \sum_{m=-\infty}^{+\infty} p(\alpha) A_m^I(\alpha) e^{-jk_m(\alpha)x} e^{-j\gamma_m(\alpha)y}. \quad (5)$$

In (5), A_m^I are the unknown coefficients of the scattered field in the upper region I; $k_m(\alpha)$ and $\gamma_m(\alpha)$ represent the propagation constants along x and y, respectively, whose expressions are defined as

$$k_m(\alpha) = \left(\frac{2\pi m}{d}\right) + \alpha \quad (6)$$

$$\gamma_m(\alpha) = \begin{cases} \sqrt{k^2 - k_m^2(\alpha)} & \text{if } k > k_m(\alpha) \\ -j\sqrt{k_m^2(\alpha) - k^2} & \text{if } k < k_m(\alpha). \end{cases} \quad (7)$$

The total scattered field $u^s(x,y)$ can be then determined as the superposition of the contributions due to each plane wave composing the incident field

$$\begin{aligned} u^s(x,y) &= \int_{-\infty}^{+\infty} U^s(x,y;\alpha)\, d\alpha \\ &= \int_{-\infty}^{+\infty} p(\alpha) \sum_{m=-\infty}^{+\infty} A_m^I(\alpha) \\ &\quad \times e^{-jk_m(\alpha)x} e^{-j\gamma_m(\alpha)y}\, d\alpha. \end{aligned} \quad (8)$$

A similar analysis holds for the transmitted field in region III, but for a sign change in γ_m.

In region II, the Helmholtz scalar equation must be solved :

$$\left[\nabla_t^2 + k_s^2(x,y)\right] U^{\rm tot}(x,y;\alpha) = 0 \quad (9)$$

where $U^{\rm tot}(x,y;\alpha)$ is the spectral component of the total field, subject to the appropriate boundary conditions, i.e., the continuity of the tangential components of the field and its normal derivatives on Γ_U and Γ_B [11]. Additionally, the periodicity of the field on Γ_L and Γ_R must hold along the x direction. Moreover, $k_s(x,y)$ is the wave number of the medium. A weighted residuals procedure can therefore be applied with identical basis and weighting functions (Galerkin's procedure). By employing a weak form of the Helmoltz equation, a FEM solution can be issued by discretizing region II into M elements where a set of first order linear basis functions $W_j^i(x,y)$ (nodal elements) is chosen for interpolating the field at the N_p nodes. The total field can be expressed as

$$U^{\rm tot}(x,y;\alpha) = \sum_{i=1}^{M} \sum_{j=1}^{N_e} v_j^i W_j^i(x,y) \quad (10)$$

where v_j^i is the field value at jth node of ith element, while N_e is the number of nodes per element.

A set of linear equations is obtained which can be written in the following matrix form:

$$\begin{bmatrix} \underline{A} & \underline{B} \\ \underline{\underline{C}} & \underline{\underline{D}} \end{bmatrix} \begin{bmatrix} \underline{V} \\ \underline{E} \end{bmatrix} = \begin{bmatrix} \underline{I} \\ \underline{P} \end{bmatrix}. \quad (11)$$

The unknown column vector $\underline{E}$ of dimension N_p contains the unknown electric field values at nodal points inside region II. The column vector $\underline{V}$ contains the values of the Floquet's coefficients in regions I and III. If the electric field in region I and region III is expanded in $2M_U + 1$ and $2M_B + 1$ harmonics, respectively, the total dimension of vector $\underline{V}$ is $2(M_U + M_B + 1)$. Submatrices of the global solving matrix assume the following meaning: $\underline{\underline{D}}$ is a band matrix representing the conventional FEM solving matrix with dimensions $N_p \times N_p$ [16]; submatrix $\underline{\underline{C}}$ accounts for the imposition of the boundary conditions (continuity of the normal derivative); sub-matrices $\underline{\underline{A}}$ and $\underline{\underline{B}}$ account for the continuity of the tangential components of the electric field. The forcing term (excitation vector) is given by the column vectors $\underline{I}$ and $\underline{P}$. The former contains only one element different from zero, i.e.,

$$I_{2M_U+1} = -e^{jy_U \sin\psi} d \quad (12)$$

(y_U is the ordinate of the boundary Γ_U), the latter exhibits nonzero values only at the N_U nodes belonging to the upper boundary.

For an exact evaluation of the field scattered by a Gaussian beam, the FEM procedure now described must be applied for each plane wave belonging to the incident field spectrum so that a large amount of plane waves must be considered. In the next section, an asymptotic procedure is devised allowing us to take into account only one specific plane wave belonging to the incident spectrum.

III. High-Frequency Approximation

In the following, we will focus on the scattered field in region I when the periodic structure is illuminated by a Gaussian beam being the treatment for the transmitted field in region III analogous. In the context of a spectral technique, we consider the complex variable $\xi = \xi' + j\xi''$ and the change of variables $\alpha = k\sin\xi$ so that (8) becomes

$$u^s(x,y) = \int_C p(\xi) \sum_{m=-\infty}^{+\infty} A_m^I(\xi) e^{-jk_m(\xi)x} \times e^{-j\gamma_m(\xi)y} k\cos(\xi)\, d\xi. \tag{13}$$

By considering real values for α, the integral is evaluated along the path C depicted in Fig. 4. Additionally, we operate in cylindrical coordinates (ρ,φ); consequently, by interchanging the sum operator with the integration, the total scattered field can be obtained as

$$u^s(\rho,\varphi) = \sum_{m=-\infty}^{+\infty} \int_C p(\xi) A_m^I(\xi) \times e^{-j\rho[k_m(\xi)\sin\varphi + \gamma_m(\xi)\cos\varphi]} k\cos(\xi)\, d\xi. \tag{14}$$

Equation (14) can be interpreted as a summation of integrals that can be separately evaluated by applying the saddle point method. In particular, if we define two functions $F(\xi)$ and $f(\xi)$

$$F(\xi) \equiv p(\xi) A_m^I(\xi) k\cos(\xi), \tag{15}$$

$$f(\xi) \equiv -j[k_m(\xi)\sin\varphi + \gamma_m(\xi)\cos\varphi] \tag{16}$$

we have for a single term

$$\int_C F(\xi) e^{\rho f(\xi)}\, d\xi = \int_{\mathrm{SDP}} F(\xi) e^{\rho f(\xi)}\, d\xi + \sum \mathrm{Res} \tag{17}$$

where $\sum \mathrm{Res}$ denotes the summation of the residues evaluated at the pole singularities lying in the complex plane region bounded by the steepest descent path (SDP) and the contour C (Fig. 4). Their contribution is not known *a priori* since $F(\xi)$ is known only numerically and not analytically; however, simple considerations on the distance at which their value is important led us to hypothesize that their effect can be neglected *a priori* if one is not interested in the field close to the interface. This specific aspect will be discussed in detail and numerically proven in the following section.

In the context of a high-frequency approximation, we note that $F(\xi)$, for the specific problem at hand, is a regular and slowly varying function in the neighborhood of the saddle points ξ_s. Consequently, by taking into account only terms of order $(k\rho)^{-1/2}$, (14) reduces to

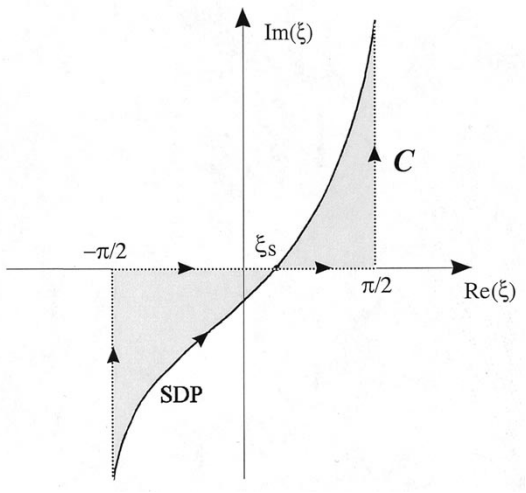

Fig. 4. Integration contour C and SDP.

$$u^s(\rho,\varphi) \approx \sum_{m=-\infty}^{+\infty} p(\xi_s) A_m^I(\xi_s) \sqrt{\frac{-2\pi\cos^2(\varphi)}{j\cos^2(\xi_s)}} k \times \cos(\xi_s) \frac{e^{-jk\rho}}{\sqrt{k\rho}} \tag{18}$$

being ξ_s the saddle points

$$\xi_s = \sin^{-1}\left[\sin(\varphi) - \frac{2\pi m}{kd}\right]. \tag{19}$$

Equation (18) can be furtherly simplified by considering that in $F(\xi_s)$ the quantity $p(k\sin\varphi - 2\pi m/d)$ is present; it approaches zero when the argument becomes large with respect to π/d, i.e., when m becomes large. This allows us to consider only the contribution of the fundamental harmonic $(m = 0)$ reducing expression (18) in the following form:

$$u^s(\rho,\theta) \approx \sqrt{\frac{-2\pi\cos^2(\varphi)}{j\cos^2(\xi_s)}} p(k\cos\psi) A_0^I(k\cos\psi) k \times \cos(\xi_s) \frac{e^{-jk\rho}}{\sqrt{k\rho}} \tag{20}$$

where $\psi = 90 - \varphi$. Equation (20) allows us to compute the field at a specific observation angle by evaluating the single contribution due to the fundamental Floquet's harmonic, this latter being the harmonic evaluated at the saddle point that coincides with the contribution in the direction of observation. It is worth noting that if a different observation angle is needed, a different saddle point (consequently, a different fundamental harmonic) must be considered.

IV. Numerical Testing and Results

We consider a 2-D photonic crystal constituted by a periodic sequence $(d = 0.46\lambda)$ of lossless dielectric rods of circular cross section with diameter $D = 0.2162\lambda$ and refractive index $n = 2$ $(\varepsilon_r = 4)$. The crystal has a hexagonal symmetry and a

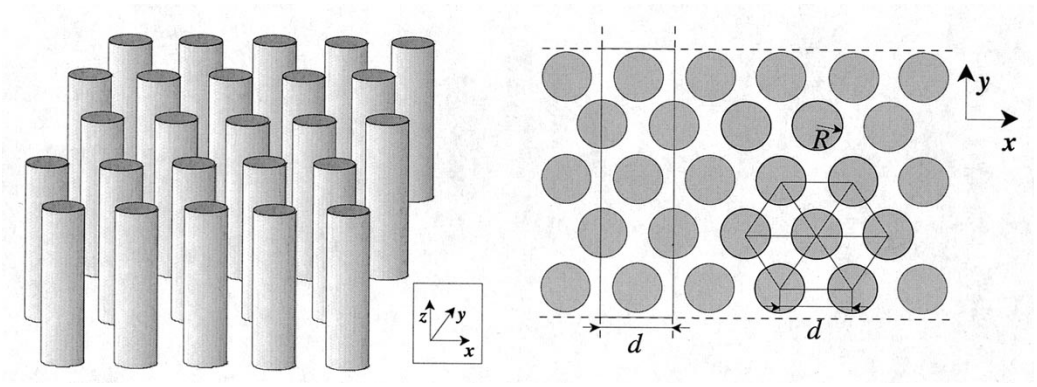

(a)

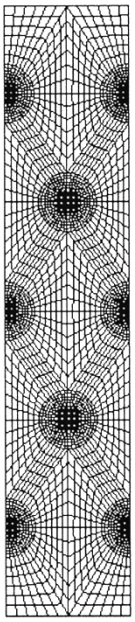

(b)

Fig. 5. Photonic crystal under investigation. (a) Geometry of a five-layer structure with dielectric cylinders ($\varepsilon_r = 4$). (b) Mesh of the bounded region of the basic periodicity cell.

five-layer structure is specifically considered [Fig. 5(a)]. The bounded region of the basic periodicity cell has been meshed by using 3312 quadrangular elements with 3433 nodes (see Fig. 5(b)). We use a very refined mesh to guarantee a precise FEM computation; in this way, the accuracy issues related to the high-frequency approximation hereafter discussed, are not affected by the specific FEM implementation employed. Moreover, the choice of quadrangular elements allows us to reduce the number of unknowns with respect to a triangular mesh.

First, the bandgap properties of the structure considered are shown in Fig. 6. In particular, the ratio of the transmitted power to the total incident power, computed by using the hybrid FEM/Floquet modes approach, is shown as a function of the frequency for a plane wave excitation with an incidence angle $\vartheta^i = 30°$. The existence of a forbidden band in the interval around $\lambda/d \approx 2$ is clearly apparent in the same figure. This result compares well with similar geometries already studied in the literature [10], confirming the accuracy of the method for what concerns a single plane wave excitation.

We consider next a Gaussian beam excitation: the results obtained by the high-frequency approximation described above are compared with the results provided by the spectral procedure that accounts for the presence of all plane waves between $[\bar{\alpha}-k, \bar{\alpha}+k]$. An exact evaluation of the incident field should include the presence of the inhomogeneous plane waves: however, in order to reduce computational costs, only the homogeneous incident plane waves have been considered; in fact, extensive numerical tests showed that the presence of these latter can be neglected without loss of accuracy. In Fig. 7, we show the reflected field evaluated at a distance of 0.22λ from the interface when the incident field has a mean incidence angle $\vartheta^i = 30°$ and a standard deviation $a = k$. The dashed line refers to the case in which $N = 1200$ plane waves (both homogeneous and inhomogeneous) in the incident field expansion are taken into account; the continuous line refers to the case in which only the homogeneous plane waves are taken into account, these latter result to be 800. As can be seen, the difference between the two cases is very small, allowing us to consider only the homogeneous plane waves in the expansion of the incident field.

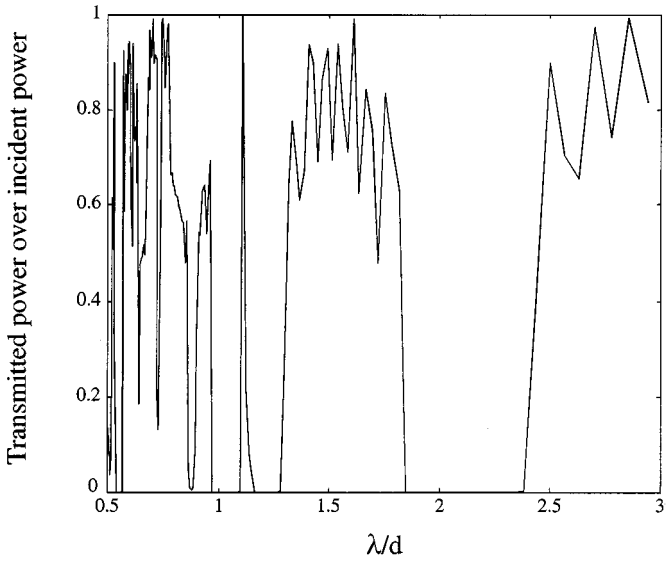

Fig. 6. Transmitted power over incident power for a plane wave excitation against the ratio λ/d. The structure is that of Fig. 5; the plane wave is incident at an angle $\vartheta^i = 30°$, TE$_z$ polarization.

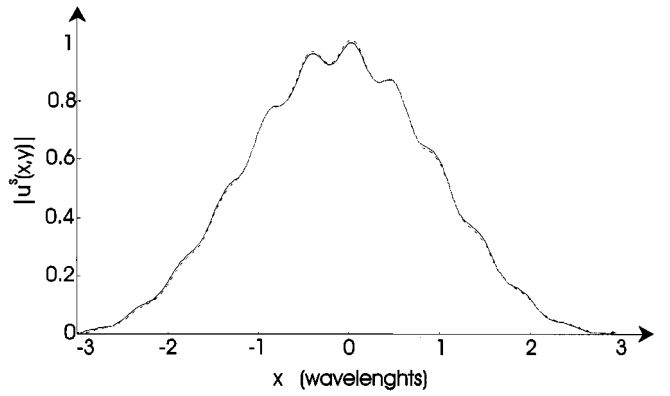

Fig. 7. Reflected field evaluated at a distance of 0.22λ from the interface for a mean incidence angle $\vartheta^i = 30°$.

It is important to highlight that the high-frequency approximation here considered can be applied to the case of photonic crystals due to the peculiarity of the function $F(\xi)$ which, as mentioned above, is regular and slowly varying in the neighborhood of saddle points in the forbidden bandgap. In Fig. 8, we show the behavior of $F(\xi)$ in the neighborhood of the saddle point for the crystal under investigation.

In the last figures we show the field scattered by the 2-D photonic crystal in Fig. 5(a) evaluated by using the asymptotic procedure previously illustrated in comparison with the value computed by employing a large number N of plane waves (this value can be viewed as exact for N becoming larger and larger). In particular, we compute the error ε as

$$\varepsilon = \frac{|u_N - u^{\mathrm{as}}|}{|u_N|} 100 \tag{21}$$

where u^{as} is the field computed by using (20) and u_N is the field evaluated by employing N plane waves in the incident field. It is worth observing that the error arising by using (20) is associated

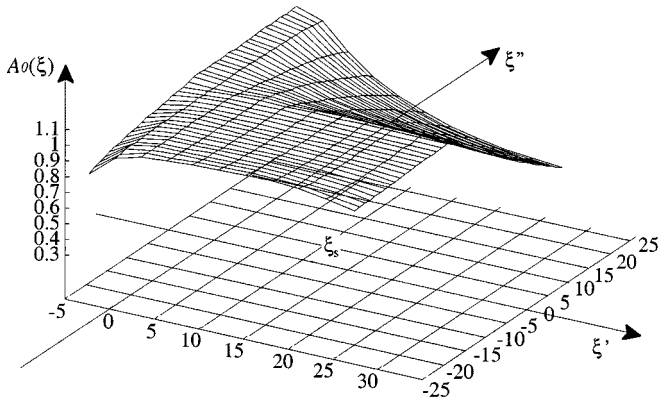

Fig. 8. Amplitude of $F(\xi)$ in the neighborhood of the saddle point for the crystal under investigation.

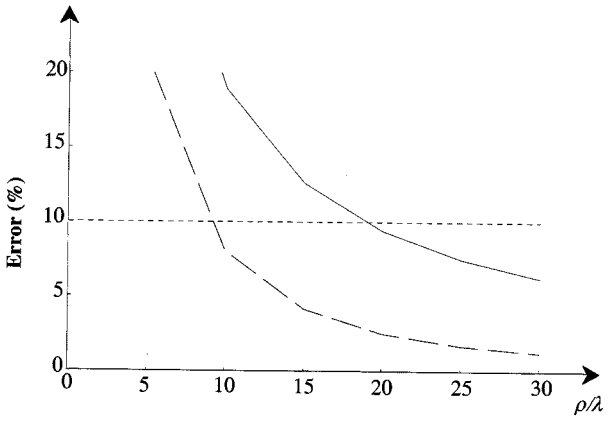

Fig. 9. Error arising in the evaluation of the reflected field from the crystal in Fig. 5 as a function of the distance from the interface. Normal incidence $\vartheta^i = 0°$, $N = 3000$. Continuous line: observation angle $\varphi = 5.7°$; dashed line: observation angle $\varphi = 9°$.

with the assumption of neglecting the residues in (17). In Fig. 9, we plot the error as a function of the distance ρ along a specific direction belonging to the -3 dB aperture of the reflected beam. This latter has been determined by evaluating the angle at which the incident field reduces of 3 dB at a fixed ρ. In particular, in Fig. 9, the case of normal incidence ($\vartheta^i = 0°$) and standard deviation $a = k$ has been considered (with the standard deviation considered above, the $-$3-dB aperture corresponds to an angle of approximately 18° symmetric along the mean incidence direction); the observation angle was set equal to $\varphi = 5.7°$ (continuous line) and $\varphi = 9°$ (dashed line) and in both cases the field has been compared with the cases of $N = 3000$ plane waves. As apparent, the error between the asymptotic procedure and the exact procedure becomes smaller and smaller for larger values of ρ. However, it is limited to 10% for $\rho = 18\lambda$ within the half-power aperture of the reflected field.

In Fig. 10, we plot the error as a function of distance but for a mean incidence angle of 30°; the observation angle was set equal to $\varphi = 26°$ (continuous line) and $\varphi = 39°$ (dashed line). The field has been again compared with data obtained by considering $N = 3000$ plane waves. In this latter case the error is limited to 10% for $\rho > 22\lambda$ within the half-power aperture of the reflected field.

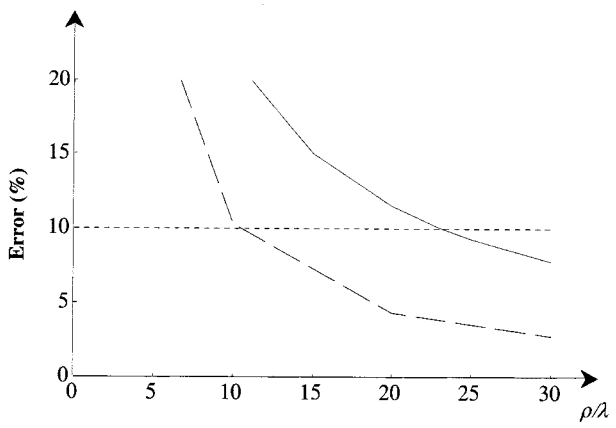

Fig. 10. Error arising in the evaluation of the reflected field from the crystal in Fig. 5 as a function of the distance from the interface. Oblique incidence $\vartheta^i = 30°$, $N = 3000$. Continuous line: observation angle $\varphi = 26°$; dashed line: observation angle $\varphi = 39°$.

Similar results have been obtained for different values of the standard deviation of the incident beam. As a general behavior, we address that the asymptotic procedure provides a good accuracy at large distances from the interface; however, the error can be maintained at a reasonable value at lower distances within the main beam of the reflected field. Depending on the specific application, a compromise between accuracy and computation time can therefore be obtained. Additionally, we note that the asymptotic procedure here presented can be efficiently employed at optical frequencies where the operative wavelengths are very small.

V. Conclusion

In this paper, we addressed the problem of the scattering of a Gaussian beam from 2-D photonic crystal. By interpreting the incident Gaussian beam as a spectrum of plane waves, the problem has been reduced to the analysis of the scattering of a plane wave, which has therefore been solved by a hybrid technique, which combines the FEM with a Floquet's modal expansion. The problem of a correct sampling of the incident field spectrum has been addressed. The influence of inhomogeneous plane waves has been numerically evaluated and it has been shown that in practical applications they can be neglected without any loss of accuracy. The bandgap properties of these structures have therefore been exploited for devising an efficient numerical solution in the high-frequency approximation by applying the saddle point method: the evaluation of the field at a specific point of the exterior medium, under Gaussian beam illumination, is reduced to the contribution of the fundamental Floquet mode due to a single plane wave belonging to the incident spectrum strongly enhancing numerical efficiency. The limits of applicability of the procedure have been discussed. The promising results obtained lead us to consider a possible extension of the method to different kinds of illuminations and scattering structures.

References

[1] E. Yablonovitch, "Photonic crystals," *J. Modern Opt.*, vol. 41, no. 2, pp. 173–194, 1994.
[2] ——, "Inhibited spontaneous emission in solid-state physics and electronics," *Phys. Rev. Lett.*, vol. 58, no. 20, pp. 2059–2062, May 1987.
[3] E. Yablonovitch, T. J. Gmitter, and K. M. Leung, "Photonic band structure: The face-centered-cubic case employing nonspherical atoms," *Phys. Rev. Lett.*, vol. 67, no. 17, pp. 2295–2298, Oct. 1991.
[4] J. D. Joannopoulos, R. D. Meade, and J. N. Winn, *Photonic Crystals: Molding the Flow of Light*. Princeton, NJ: Princeton Univ. Press, 1995.
[5] H. Y. D. Yang, "Finite difference analysis of 2-D photonic crystals," *IEEE Trans. Microwave Theory Tech.*, vol. 44, pp. 2688–2695, Dec. 1996.
[6] M. P. Kesler, J. G. Maloney, B. L. Shirley, and G. S. Smith, "Antenna design with the use of photonic band-gap materials as all-dielectric planar reflectors," *Microwave Opt. Technol. Lett.*, vol. 11, no. 4, pp. 169–174, Mar. 1996.
[7] E. R. Brown and O. B. McMahon, "High zenithal directivity from a dipole antenna on a photonic crystal," *Appl. Phys. Lett.*, vol. 68, no. 9, pp. 1300–1302, Feb. 1996.
[8] H.-Y. D. Yang, N. G. Alexopoulos, and E. Yablonovitch, "Photonic bandgap materials for high-gain printed circuit antennas," *IEEE Trans. Antennas Propagat.*, vol. 45, pp. 185–186, Jan. 1997.
[9] D. Maystre, G. Tayeb, and D. Felbacq, "Electromagnetic study of photonic band structures and Anderson localization," in *Quantum Optics in Wavelength Scale Structures*, J. G. Rarity and C. Weisbuch, Eds, Dordrecht, The Netherlands: Kluwer, 1996.
[10] D. Maystre, "Electromagnetic study of photonic band gaps," *Pure Appl. Opt.*, vol. 3, pp. 975–993, 1994.
[11] G. Pelosi, A. Freni, and R. Coccioli, "Hybrid technique for analysing scattering from periodic structures," *Proc. Inst. Elect. Eng.*, pt. H, vol. 140, no. 2, pp. 65–70, Apr. 1993.
[12] G. Pelosi, R. Coccioli, and S. Selleri, *Quick Finite Element for Electromagnetic Waves*. Norwood, MA: Artech House, 1998, pp. 115–131.
[13] P. C. Clemmow, *The Plane Wave Spectrum Representation of Electromagnetic Fields*. Piscataway, NJ: IEEE Press, 1996.
[14] G. Pelosi and R. Coccioli, "A finite element approach for scattering from inhomogeneous media with a rough interface," *Waves Random Media*, vol. 7, pp. 119–127, 1997.
[15] C. G. Mias, "Finite element modeling of the electromagnetic behavior of spatially periodic structures," Ph.D. dissertation, Univ. Cambridge, U.K., 1995.
[16] P. P. Silvester and R. L. Ferrari, *Finite Elements for Electrical Engineers*, 3rd ed. Cambridge, MA: Cambridge Univ. Press, 1996.

Giuseppe Pelosi was born in Pisa, Italy. He received the Laurea (Doctor) degree in physics (*summa cum laude*) from the University of Florence, Italy, in 1976.

Since 1979, he has with the Department of Electronic Engineering, University of Florence, where he is currently a Full Professor of Microwave Engineering. He was a Visiting Scientist at McGill University, Montreal, Canada in 1994 and 1995. He is coauthor of *Finite Elements for Wave Electromagnetics* (New York: IEEE Press, 1994), *Finite Element Software for Microwave Engineering* (New York: Wiley, 1996) and *Quick Finite Elements for Electromagnetic Fields* (Norwood, MA: Artech House, 1998). He has been mainly involved in research in the field of numerical and asymptotic techniques for applied electromagnetics. His past research have extensions and applications to the geometrical theory of diffraction as well as methods for radar cross section analysis of complex targets. His current research activity is mainly devoted to the development of numerical procedures in the context of the finite-element method, with particular emphasis on microwave and millimeter-wave engineering (antennas, circuits, devices, and scattering problems).

Dr. Pelosi is a member of the board of the directors of the Applied Computational Electromagnetics Society.

Alessandro Cocchi was born in Florence, Italy, on October 24, 1970. He received the Laurea (Doctor's) degree in electronics engineering from the University of Florence, Italy, in 1997.

He first collaborated with the Department of Electronics and Telecommunications of the University of Florence, where was involved in research in the field of numerical methods for applied electromagnetics and radiated problems. He is currently with the Officine Galileo, Florence, Italy, where he is a Research Engineer in infrared image processing.

Agostino Monorchio (S'89–M'96) was born in Italy, March 16, 1966. He received the Laurea (electronics engineering) and the Ph.D. (methods and technologies for environmental monitoring) degrees, from the University of Pisa, Italy, in 1991 and 1994, respectively.

In 1995, he joined the Radio Astronomy Group at the Arcetri Astrophysical Observatory, Florence, Italy, as a Postdoctoral Research Fellow, working in the area of microwave systems. Since January 1997, he has been collaborating with the Electromagnetic Communication Laboratory, Pennsylvania State University, State College, PA, first as a Visiting Scholar and then as an Adjunct Member. He is currently an Assistant Professor in the School of Engineering, University of Pisa. His research interests include numerical and asymptotic methods for applied electromagnetics in both frequency and time domains. He has also been involved in research related to the analysis of frequency selective surfaces and the definition of electromagnetic models of scattering from the sea surface for remote sensing applications.